Earth and Planetary Science Letters 277 (2009) 443–452

Contents lists available at ScienceDirect

Earth and Planetary Science Letters

journal homepage: www.elsevier.com/locate/epsl

Strengthened East Asian summer monsoons during a period of high-latitude warmth? Isotopic evidence from Mio-Pliocene fossil mammals and soil carbonates from northern China

Benjamin H. Passey [a,*], Linda K. Ayliffe [a,b], Anu Kaakinen [c], Zhaoqun Zhang [d], Jussi T. Eronen [c], Yanming Zhu [e], Liping Zhou [e], Thure E. Cerling [a], Mikael Fortelius [c,f]

[a] Department of Geology and Geophysics, University of Utah, 135 S. 1460 E. Rm. 719, Salt Lake City, UT 84112, USA
[b] Research School of Earth Sciences, The Australian National University, Canberra, ACT, 0200, Australia
[c] Department of Geology, P.O. Box 64 (Gustaf Hällströmin katu 2a) FIN-00014 University of Helsinki, Finland
[d] Institute of Vertebrate Paleontology and Paleoanthropology, Chinese Academy of Sciences, Beijing 100044, China
[e] Laboratory for Earth Surface Processes, Department of Geography, Peking University, Beijing 100871, China.
[f] Institute of Biotechnology, P.O. Box 64 (Gustaf Hällströmin katu 2a) FIN-00014 University of Helsinki, Finland

ARTICLE INFO

Article history:
Received 27 June 2008
Received in revised form 27 October 2008
Accepted 10 November 2008
Available online 5 December 2008

Editor: P. deMenocal

Keywords:
East Asian monsoon
C_4 vegetation
stable isotopes
fossil tooth enamel
summer monsoon

ABSTRACT

The East Asian monsoons have fluctuated in concert with high-latitude warmth during the past several hundred thousand years, with humid summer monsoon-dominant climates characterizing warm intervals, including interglacials and interstadials, and arid winter monsoon-dominant climates characterizing cool intervals, including glacials and stadials. Of the states comprising the mid-Pleistocene to recent climatic regime, interglacials are most similar in terms of high latitude ice volumes and temperatures to those extant during the late Miocene and early Pliocene. Thus, an important question is whether Mio-Pliocene climates in northern China were analogous to a hypothetical 'prolonged interglacial state,' with increased summer monsoon precipitation and expansion of forest and steppe environments at the expense of desert environments.

We utilize new and previously published carbon isotopic data from fossil teeth and soil carbonates to place constraints on paleovegetation distributions and to help infer the behavior of the monsoon system between ~7 and 4 Ma. We find that plants using the C_4 photosynthetic pathway—which today are largely grasses found in regions with warm season precipitation—were present in northern China by late Miocene time, demonstrating that the C_4 expansion in China was not significantly delayed compared to the global C_4 event. During the late Miocene–early Pliocene interval, soil carbonate and tooth enamel $\delta^{13}C$ data indicate: 1) that nearly pure C_3-plant ecosystems existed in the southern Chinese Loess Plateau (CLP), and therefore ecosystems there were dominated by woody dicot, herbaceous dicot, or cool-season grass vegetation (or a combination of these), and 2) that the CLP was characterized by a pattern of northward-increasing C_4 vegetation and aridity. Utilizing a broadened conceptual model for interpreting $\delta^{13}C$ data, and citing independent faunal, floral, and lithostratgraphic data, we suggest that these patterns reflect northward expansion of forest and steppe ecosystems and relatively humid monsoon climates during the late Miocene and early Pliocene. An important implication of this interpretation is that the forcing mechanism illuminated by the temporal correlation during the Pleistocene between warm high latitudes and strong East Asian summer monsoons is a robust feature of the Eurasian tectonic–climatic system that predates the Plio-Pleistocene climatic reorganization.

1. Introduction

The East Asian monsoon (EAM) dominates the climate over much of China and the surrounding region, and is the primary moisture source for a large fraction of the human population. The system is characterized by a seasonal switching between winter monsoons (EAWM) that bring cold, dry air and occasional dust storms from the northwest, and summer monsoons (EASM) that bring warm air and moisture from the southeast. Interior regions, such as the Chinese Loess Plateau (CLP), receive the majority of precipitation during the warm summer months. The strength of the EASM decreases to the northwest, and this controls the distribution of vegetation: forest is the dominant physiognomy in southeastern China, and this gives way to steppe and ultimately desert environments in northwestern China. The CLP is presently located within this transition zone (Fig. 1), and is ideally situated for studying long-term fluctuations in monsoon climate.

* Corresponding author. Present address: Division of Geological and Planetary Sciences, California Institute of Technology, MC 100-23, 1200 E. California Blvd., Pasadena, CA 91125, USA.
E-mail address: bhpassey@gps.caltech.edu (B.H. Passey).

0012-821X/$ – see front matter © 2008 Elsevier B.V. All rights reserved.
doi:10.1016/j.epsl.2008.11.008

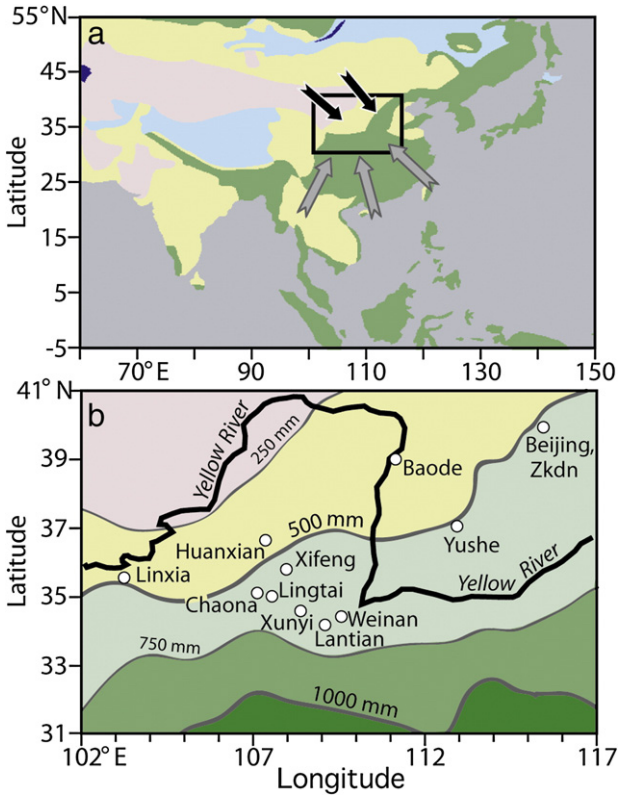

Fig. 1. Location maps showing general climatic and ecological features of the study area. (a) Ecoregions and generalized transport directions for summer (gray arrows) and winter (black arrows) monsoons over eastern Asia. The ecoregions (Bailey, 1989/1993) are grouped as follows: green, forests; yellow, transitional, including savanna, open woodland, and steppe; pink, desert and desert-steppe; light blue, tundra and high-elevation cold desert; dark blue, inland water. (b) Detail of the Chinese Loess Plateau region, showing localities discussed in the text and figures, and mean annual precipitation contours (UCAR, 2006). Zkdn: Zhoukoudian. (For interpretation of the references to colour in this figure legend, the reader is referred to the web version of this article.)

There is much debate concerning the timing of onset, and the subsequent history, of the EAM. Climate models show that a high elevation (>3000 m) Tibetan Plateau helps to drive strong monsoonal circulation in this region (Kutzbach et al., 1993, An et al., 2001, Zhang et al., 2007). Proxy records from land and sea show a number of changes during the latest Miocene that are suggestive of increased monsoonal circulation for both the Indian and East Asian monsoons (Molnar, 2005). Paleobotanical and sedimentological evidence suggests that a monsoon-like climatic pattern was in place in East Asia by the early Miocene (Guo et al., 2002; Sun and Wang, 2005). However, high resolution magnetic susceptibility, Rb/Sr, and grain size records from the Loess Plateau have been interpreted as indicating relatively weak summer and winter monsoons in China prior to ~3.6 Ma (An et al., 2001, 2005). Published carbon isotope records from Loess Plateau soil carbonates suggest that C_4 plants were unimportant prior to ~3.6 Ma, leading workers to further conclude that the EASM was relatively weak prior to this time (Ding and Yang, 2000, Jiang et al., 2002, An et al., 2005). This view has been additionally supported by tooth enamel carbon isotope data from China showing no evidence for C_4 vegetation in herbivore diets prior to the Pleistocene (Wang and Deng, 2005).

This 'weak Mio-Pliocene EASM' interpretation is somewhat surprising given the Pleistocene history of the monsoons in the context of global-scale climatic variability. A clear link has emerged between strengthened EASM circulation and 'warm' intervals in the high latitude Northern Hemisphere. Intensive study of the loess–paleosol strata of the CLP during the past two decades has revealed that this pattern existed throughout the Pleistocene (e.g., Liu and Ding, 1998, An, 2000, Hao and Guo, 2005), with soils (now paleosols) developing during warm-humid interglacial climates, and wind-blown loess accumulating during cool-arid glacial climates. The dominant frequency in the loess–paleosol strata, like that in the global ice volume record, changes from an ~40 ka-dominant signal to an ~100 ka-dominant signal during the mid-late Pleistocene (Liu and Ding, 1998). Since the primary Milankovitch forcing does not reside in the 100 ka band (Imbrie et al., 1992), this suggests that the EAM is also sensitive to parameters other than insolation, including high-latitude climate and ice volume. More recently, high-resolution speloethem records from central and northern China have shown that the EASM during the past 220 ka varied in phase with high latitude summer insolation, and that the EASM also strengthened in concert with high latitude millennial-scale warming events (Wang et al., 2008). Therefore the Pleistocene EASM appears to strengthen during warm intervals in the high latitudes, regardless of whether these are driven by orbital or nonorbital phenomena.

While the orbital parameters of the late Miocene and early Pliocene were similar to those of the Pleistocene, this interval was globally much warmer, especially in the high latitudes, and featured reduced ice volume compared to today (Dowsett et al., 1994; Mix et al., 1995; Ravelo et al., 2004). Thus it might be predicted—using an uniformitarian approach with the Pleistocene system as the key to earlier systems—that the Mio-Pliocene was characterized by relatively strong EASM circulation in a climatic state perhaps similar to a prolonged Pleistocene interglacial. Indeed, the qualitative impression given by the bulk characteristics of the eolian 'red clay' strata accumulated in the CLP during this interval, including fine grain size, low deposition rate, and strong pedogenesis (Ding et al., 1998, 1999; Sun et al., 2006), is one of relatively humid climates. The recent suggestion of relatively weak Mio-Pliocene EASM, based largely on interpretations of CLP magnetic susceptibility, Rb/Sr, and C_4 vegetation records (An et al., 2001, 2005; Wang and Deng, 2005), clearly calls this notion into question. If this latter interpretation is correct, an important implication is that the monsoon system underwent a fundamental change during the Plio-Pleistocene transition, such that its present behavior is not a particularly good key to its past behavior.

There is some controversy about the paleoclimatic significance of magnetic susceptibility in the Mio-Pliocene red clay strata of the CLP. The correlations among strengthened EASM, increased soil development, and enhanced magnetic susceptibility observed in the late Pleistocene loess–palaeosol strata originally prompted workers to extend the magnetic susceptibility record (and related indices such as Rb/Sr ratio; Chen et al., 1999) into the underlying red clay strata as proxies of summer monsoon strength (An et al., 1999, 2001). However, this interpretation of magnetic susceptibility in the red clay remains to be rigorously justified, and recent studies have questioned the assumption that these parameters have coherency across stratigraphic columns encompassing different modes of sedimentation and pedogenesis (e.g., Bloemendal et al., 2008).

This paper continues the exploration of the late Neogene history of C_3 and C_4 plants in northern China, with the goal of gaining a better understanding of the ecological and climatic evolution of this region. C_4 vegetation is useful in reconstructing past bioclimates because the ratio of C_4 grass to C_3 grass in open ecosystems is primarily controlled by growing season temperature (Teeri and Stowe, 1976). C_3 and C_4 plants have distinct $^{13}C/^{12}C$ ratios, and this distinction is preserved in fossil soil organic matter, carbonate, and tooth enamel, enabling the study of ancient C_3 and C_4 vegetation distributions (Koch, 1998; Kohn and Cerling, 2002). In the modern environment, crossover temperatures in terms of C_3/C_4 species ratio range between 20 and 28°C for growing season temperature (see compilation in Ehleringer et al., 1997), with the exact values varying due to environmental factors and partially obscured by the use of different temperature parameters by different authors. Correlation coefficients (r, R^2) for regressions between C_3/C_4 species ratio and temperature are typically >0.9 (Ehleringer et al., 1997). C_4

grasses are the dominant grass type in low latitudes and in temperate regions with summer monsoon climates, whereas C_3 grasses are found in high latitudes and in regions with Mediterranean climates. Most trees, shrubs, and other dicots utilize the C_3 pathway, and forest ecosystems therefore have a C_3 carbon isotope signature. In regions with C_4 grass vegetation, the C_3/C_4 distinction can be utilized to track changing distributions of wooded and grassy habitats (West et al., 2000).

In this paper, we present new carbon isotope data from fossil mammals and soil carbonates from northern China that provide, along with previously published data, a temporally and spatially resolved history of C_4 plants in this region. The tooth enamel data ($n=135$) are from fossil herbivores from the Baode, Yushe, and Lantian localities in the CLP, and range in age from ~10 to 2 Ma. The soil carbonate carbon isotope data ($n=147$) are from the red clay Baode Formation near Baode, Shanxi Province (Fig. 1), and span ~7.3 to 5.3 Ma. After presenting the data, we examine latitudinal trends in soil carbonate and tooth enamel $\delta^{13}C$, and offer an alternative scenario of Neogene climate history that is consistent with these observations. We conclude with a discussion of independent climate proxy data in the context of this proposed climate history, and implications for the long-term forcing of the East Asian monsoons.

2. Setting, materials, and methods

2.1. Geological and climatic setting

Late Neogene sediments in the CLP are dominated by two widespread units, the 'red clay,' and the overlying loess–paleosol sequences, and both are primarily eolian in origin (An, 2000; Ding et al., 1998). Together these units comprise a virtually continuous sedimentary record spanning from the present day to 7–8 Ma, but locally extending back to ~22 Ma (Guo et al., 2002). The transition from red clay to loess–paleosol takes place approximately 2.7 Ma ago, coincident with the intensification of Northern Hemisphere glaciation (An et al., 2001).

The climate in the CLP is semiarid to arid, and the EAM controls the distribution of precipitation. The rainy season is primarily between June and September, during which more than two-thirds of the annual precipitation falls. Mean annual precipitation (MAP) ranges from 500 to 600 mm in the southern plateau to 300 mm or less in the northern plateau (Fig. 1b). Mean annual temperature (MAT) is typically 12–14 °C in the southern plateau and 6–8 °C in the northern plateau (UCAR, 2006).

The patterns of vegetation in this region mirror the patterns of precipitation. Broadleaf deciduous forest is dominant to the south of the CLP, and the CLP spans the transition from steppe in the southeast, to desert in the northwest (Hou, 1983). C_4 vegetation is an important component of biomass in the loess plateau, and its abundance increases with increasing growing season precipitation ($R^2=0.70$) and temperature ($R^2=0.41$) in this region (An et al., 2005).

2.2. Materials and methods

Fossil herbivore samples are from the well-known Bahe Fauna (Lantian), Baode Fauna (Baode), and various faunas at the Yushe localities (Qiu and Qiu, 1995). The taxa are primarily from the families Equidae, Rhinocerotidae, Giraffidae, Cervidae, and Bovidae. The age assignments of samples are based on existing biostratigraphic and magnetostratigraphic frameworks, as follows: Lantian: Kaakinen (2005), Kaakinen and Lunkka (2003); Baode: Zhu et al. (2008); Yushe: Flynn et al. (1997), Tedford et al. (1991). A small number of the tooth enamel data (12 of 135) were published in Passey et al. (2007), and these data are noted in Supplementary Table 2. Two red clay stratigraphic sections in the Baode Formation, YJG-I and YJG-II, were excavated, logged, and sampled for soil carbonates in September 2004. These correspond to the magnetostratigraphic sections of Zhu et al. (2008). Soil carbonate samples were selected from strata with clear indicators of soil development, including bioturbation, ped structure, and lack of primary laminae and beds. Tooth enamel and soil carbonates were sampled by abrading specimens with diamond- and carbide-tipped drills and collecting the resulting powder over weighing paper. Tooth enamel was pretreated in 3% H_2O_2 and 0.1 M buffered CH_3COOH, whereas carbonate samples were roasted at 200–300 °C prior to analysis. Enamel and carbonates were reacted in 100% H_3PO_4 at 90 °C in a Finnigan Carboflo common acid bath apparatus. The evolved CO_2 was cryogenically purified, and analyzed on a Finnigan MAT 252 isotope ratio mass spectrometer. Isotope values were normalized relative to in-house standards calibrated against NBS-19 carbonate reference material. Predicted $\delta^{13}C$ values for tooth enamel and soil carbonate associated with C_3 and C_4 vegetation end members are based on a compiled marine benthic foraminifera $\delta^{13}C$ record (Zachos et al., 2002) and estimates for carbon isotopic fractionations among foraminifera, atmospheric CO_2, plant biomass, soil carbonates, and tooth enamel (Passey et al., 2002), and are given in Supplementary Table 1.

3. Results

3.1. Tooth enamel

Tooth enamel $\delta^{13}C$ data are reported in Supplementary Table 2 and are illustrated in Fig. 2. Herbivores at Lantian had C_3-based diets, although 6 of the 55 individuals have $\delta^{13}C$ values suggesting a very small component of C_4 vegetation (representing ~10% or less of metabolized food). At Baode, diets were also C_3-based, but 20 of 47 individuals have $\delta^{13}C$ values reflective of a significant C_4 grass component, typically

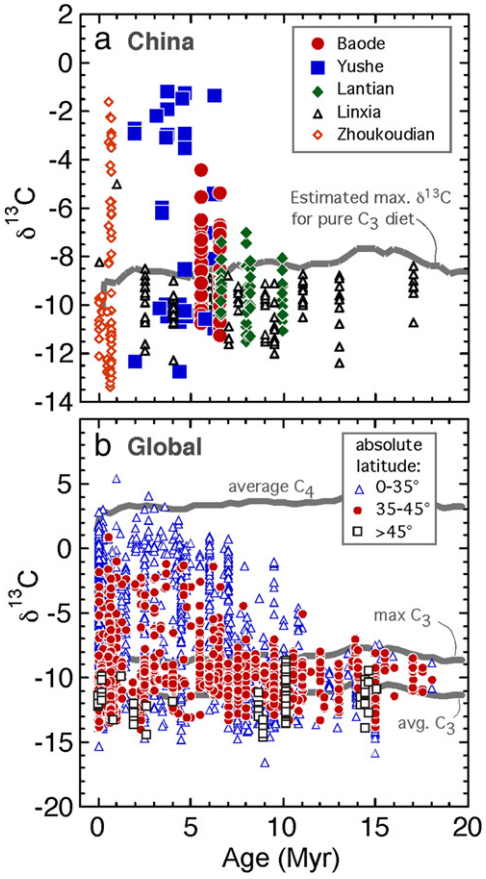

Fig. 2. Fossil tooth enamel $\delta^{13}C$ records. (a) The record from China. (b) The global record. The gray lines are model-predicted values for animals with pure C_3 diets or C_4 diets that account for changes in the $^{13}C/^{12}C$ composition of atmospheric CO_2 through time (see text and Supplementary Table 1). The Linxia and Zhoukoudian data are from Wang and Deng (2005) and Gaboardi et al. (2005), respectively. The global record was compiled from the literature and also includes unpublished data.

consisting of less than ~10%, but up to about ~30%. The C_4 signal is greatest at Yushe, with individuals commonly consuming >50% C_4 vegetation. In terms of temporal patterns, very few (4 of 54) pre-7 Ma individuals consumed C_4 vegetation, whereas after 7 Ma, C_4 vegetation was a common dietary component (39 of 94 individuals). In terms of taxonomy, equids, rhinos, and bovids commonly consumed C_4 vegetation, whereas cervids and giraffids do not show clear evidence of dietary C_4 vegetation. Tooth enamel $\delta^{18}O$ values are reported in Supplementary Table 2 but are not discussed in this paper.

3.2. Baode sedimentology and soil carbonates

The sediments at Baode are dominated by clay and silt grain sizes, with infrequent channel conglomerates (Fig. 3). There are very few horizons dominated by sand. The sediments show semi-regular cycles idealized by reddish clays grading into brown-yellow silts. Within these silts, calcium carbonate increases upward to form laterally continuous calcrete horizons ranging in thickness from 10 to 150 cm. These are overlain by the next sedimentary cycle, beginning with reddish clays, and the contact between these is usually sharp. Each cycle is 1–3 m thick, and may be complete or incomplete. The reddish clays are commonly free of carbonate, or have leached matrix with thin mm-scale wisps and veinlets of carbonate. The brown-yellow silts typically contain diffuse carbonate. Nearly all units show signs of bioturbation. In the reddish clays, ped structure is often well developed, and submillimeter flecks of authigenic, presumably Mn-bearing minerals, are common. Primary bedding and laminations are rare except in channel conglomerates. The clay-silt-carbonate units are laterally continuous on a scale of tens to hundreds of meters, whereas the channel conglomerates, which cut into these, are typically 10 m or

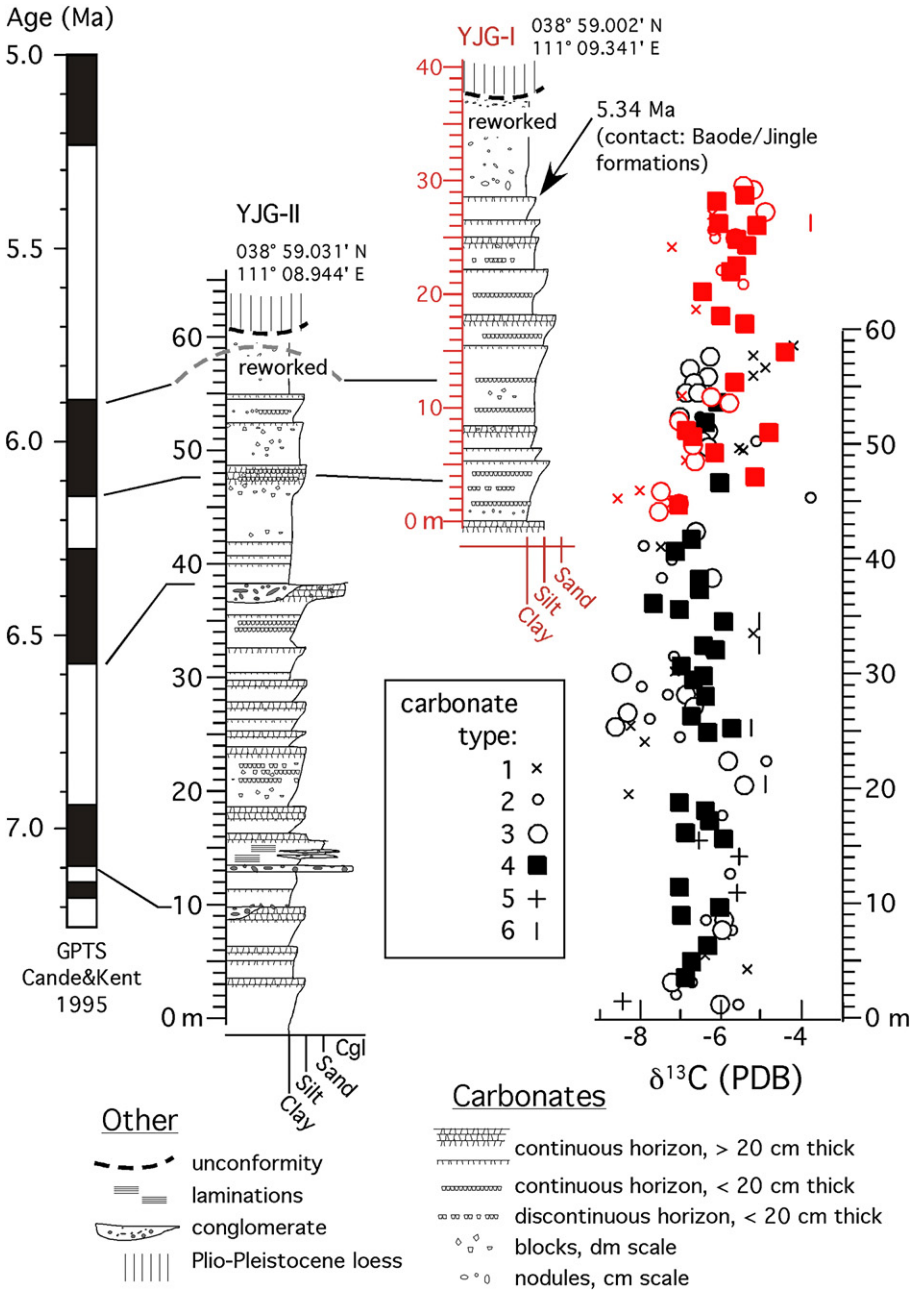

Fig. 3. Stratigraphy and $\delta^{13}C$ record from soil carbonates at Baode. Age estimates are based on magnetic reversal stratigraphy (Zhu et al., 2008). The $\delta^{13}C$ data from the YJG-I section are shown in red and are plotted on the red scale to the left, whereas the YJG-II data are shown in black and plotted on the scale to the right. The soil carbonate types are explained in section 3.2. (For interpretation of the references to colour in this figure legend, the reader is referred to the web version of this article.)

less in width. The majority of conglomerate clasts are derived from older sedimentary rocks (Mesozoic or Paleozoic), or crystalline rocks.

Stable isotopic compositions and weight percent carbonate data are reported in Supplementary Table 3. The carbonate-bearing rocks that were analyzed for stable carbon isotopes can be divided into 6 categories. Type 1 carbonates are mm-scale carbonate wisps, veinlets, and diffuse carbonate found in reddish clays, and have a median carbonate content of 3% by weight. Type 2 carbonates are diffuse carbonate in brown-yellow silts with a median carbonate content of 8%. Type 3 carbonates are indurated nodules and blocks of micritic carbonate with a median carbonate content of 49%. Type 4 carbonates are similar in hand-specimen to Type-3 carbonates, but are in-situ carbonate horizons, ranging in thickness from 10 to 150 cm. They have mottled or massive textures, and a median carbonate content of 41%. Type 5 carbonates are sediments with obvious primary bedding or laminations, including conglomerates. Finally, Type 6 carbonates are sparite crystals, typically mm-scale, that are sometimes found in Type 3 and 4 carbonates, and that are often line the walls of pockets and vugs. These are nominally 100% carbonate, but reported weight percents (Supplementary Table 3) are lower when separates were impure mixtures of spar and sediment. Types 1, 2, and 4 carbonates may grade into one another.

Except for Type 6 carbonates, the different carbonate types at Baode are indistinguishable in average $\delta^{13}C$ and $\delta^{18}O$, but differ in variability. Type 1 carbonates average −6.7±1.3 and −9.3±0.8‰ in $\delta^{13}C$ and $\delta^{18}O$, respectively (± values are 1σ). Type 2 carbonates average −6.5±1.0 and −8.9±0.9‰, Type 3 carbonates average −6.6±0.9 and −9.4±0.6‰, while Type 4 carbonates average −6.3±0.7 and −9.3±0.4‰. Type 5 carbonates average −6.5±1.3 and −8.8±0.7‰. Finally, Type 6 carbonates have a composition different from the other types, averaging −4.8±0.6 and −8.9±0.2‰. Thus, for carbon isotopes, there is a clear decrease in variability between the carbonate-poor Types 1 and 2 lithologies and the carbonate-rich Types 3 and 4 lithologies. Inference of percent C_4 vegetation from these carbonate isotope data is discussed below.

4. Discussion

4.1. Late Neogene history of C_4 vegetation in China based on tooth enamel

Wang and Deng (2005) observed essentially pure C_3 diets in herbivores from Linxia during the past 25 Ma (Fig. 2a), with the exception of one Pleistocene *Equus* individual that had significant C_4 biomass in its diet. These workers suggested that the summer monsoon in northern China, which today enables growth of C_4 vegetation, did not strengthen to levels necessary for significant C_4 vegetation until Pleistocene time. In contrast, data from this study show that C_4 vegetation was a common component of herbivore diets at Baode, Yushe, and to a lesser extent Lantian, beginning in late Miocene time. The Yushe data, along with Pliocene and Pleistocene data from other localities in northern China (Deng et al., 2002; Gaboardi et al., 2005) demonstrate the continued presence and importance of C_4 vegetation in this region following late Miocene time. The tooth enamel record in northern China is similar to that at similar latitudes in North America and elsewhere (Wang et al., 1994; Cerling et al., 1997; Passey et al., 2002) in that a small portion of late Miocene individuals consumed significant (>30%) C_4 vegetation, and that C_4 feeding continued and increased during subsequent time (Fig. 2b). Therefore, these relatively high-latitude regions record an initial late Miocene C_4 event broadly similar in timing to that observed on other continents, and slightly delayed compared to the event at lower latitudes (Fig. 2b, and Cerling et al., 1997), but not a post-Miocene event as previously understood (Wang et al., 1994; Cerling et al., 1997; Wang and Deng, 2005).

In China, the combined temporal and spatial pattern of C_4 vegetation may shed light on past climate systems. The modern summer monsoon is strongest in the southeast, and weakens to the northwest. C_4 vegetation, primarily comprised of grasses, and requiring warm temperatures during the growing season, is concentrated in a steppe zone bounded by monsoon forest to the south and desert to the north. In the context of this model, Baode, Yushe and Zhoukoudian may have been located in this C_4 maximum zone during late Miocene and subsequent time. Lantian, located to the south of these localities, records very little C_4 vegetation and may have been located in a relatively closed environment during late Miocene time.

Linxia, which resides on the western margin of the CLP region, records C_3 habitats for most of the late Neogene. This lack of C_4 vegetation compared to other localities is somewhat perplexing, though Linxia presently resides in a region where the transition between forest environments to the south and desert environments to the north is narrow compared to the transition zone in more easterly parts of the CLP. The present day elevation at Linxia is ~2000 m, and is significantly higher than any of the other localities discussed here, which are ~1300 m or lower. A relatively high paleoelevation would favor C_3 vegetation over C_4 vegetation, and orographically-enhanced precipitation would favor forest environments over steppe environments. On the other hand, it is possible that Linxia resided at a lower elevation in the past, in which case slightly different patterns of precipitation compared to the present day may have imposed dry, desert-like conditions, or humid forest-like conditions, each conducive to the growth of C_3 vegetation.

4.2. Interpretation and implications of Loess Plateau soil carbonates

4.2.1. Soil carbonates at Baode

The soil carbonates at Baode differ from soil carbonates typically used in paleoclimate reconstruction (e.g., Siwalk-type soil carbonates; such as those described in Quade et al., 1995). These are typically discrete cm-scale carbonate nodules recovered from soils with leached parent material, and collected at depth in the soil horizon (typically >50 cm) to avoid sampling material formed under the influence of atmospheric CO_2 (Cerling, 1984). Furthermore, the soils from which these nodules derive usually form on relatively static, non-accumulating, interfluve surfaces. Soil development proceeds for a finite period of time, with dissolution and leaching of parent material carbonate and other minerals in the upper horizons and precipitation of carbonate in the lower horizons. Ultimately, the soil is extinguished by burial during a subsequent sedimentary cycle.

In contrast, soil carbonates at Baode are typically massive and lacking in texture indicative of coalesced carbonate nodules. They are fractured on a dm-scale, possibly owing to penetration by large roots, and they lack the laminations and brecciation commonly found in Stage IV and V soil carbonates (Gile et al., 1966; Machette, 1985). Eolian sediment was periodically added at the surface, so that the soil surface moved upward and gradually abandoned underlying soils. Thus, any part of the soil profile may have at one time resided in a zone of leaching, and at another in a zone of carbonate accumulation. It is unclear at Baode where the soil surface was located during the time-averaged period of formation of each carbonate horizon.

In order for soil carbonates to record the isotopic composition of paleovegetation, they must be authigenic, and must have formed in equilibrium with soil CO_2 derived from plant respiration and the oxidation of plant debris (Cerling, 1984). At Baode, the Type 3 and Type 4 carbonates, with ~45% carbonate, mottled or massive texture (not bedded), and good induration, are clearly authigenic and are typically overlain by leached reddish clays. The average depths of carbonate formation, and rates of soil CO_2 production, are less clear. In the case that the soil carbonates formed close to the surface or under low soil respiration rates, and with incomplete leaching of parent material carbonate, they will have elevated $\delta^{13}C$ values compared to carbonates forming in equilibrium with C_3 vegetation. Therefore, the carbonates will appear to record more C_4 vegetation than was actually present. For this reason, estimates of percent C_4 biomass based on Baode Formation soil carbonates should be regarded as maximum values.

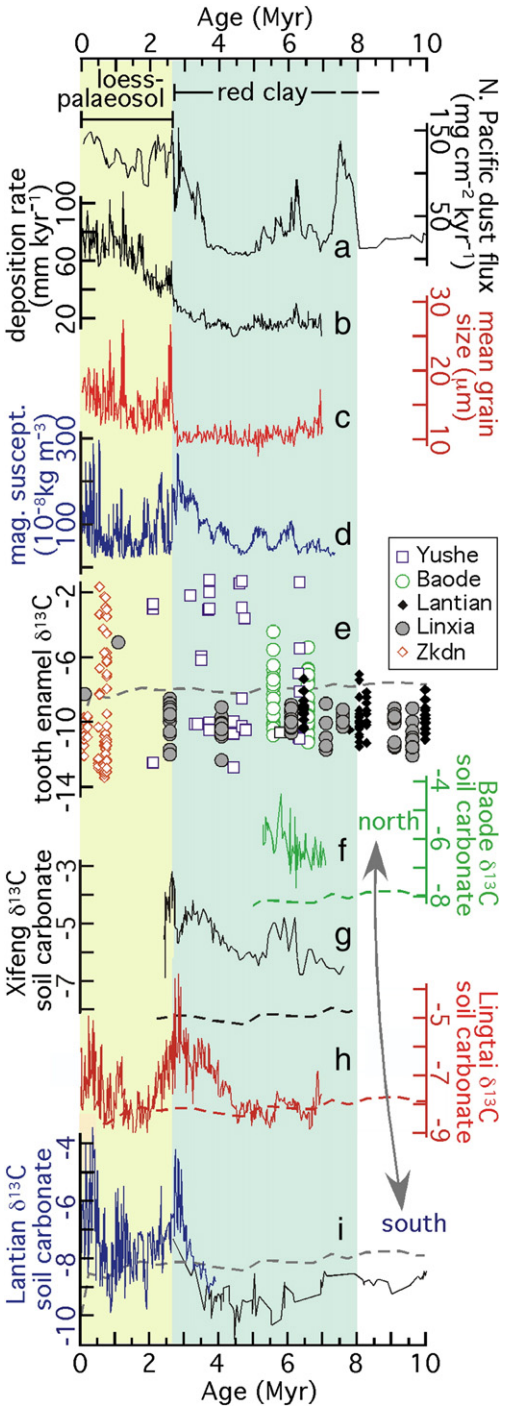

Fig. 4. Proxy records of climatic and ecological changes in northern China during the past 10 Ma. (a) Dust flux at Northern Pacific site 885/886 (Rea et al., 1998). (b) Sediment deposition rate averaged for several localities in the Chinese Loess Plateau (An et al., 2005). (c, d) Bulk sediment mean grain size and magnetic susceptibility at Lingtai (Sun et al., 2006). (e) $\delta^{13}C$ values of fossil herbivore tooth enamel from Baode, Yushe, and Lantian (this study; Supplementary Table 2), with data from Linxia (Wang and Deng, 2005) and Zhoukoudian (Gaboardi et al., 2005). (f–i) Soil carbonate $\delta^{13}C$ records from Baode (this study, Supplementary Table 3; plotted are type 4 carbonates only), Xifeng (Jiang et al., 2002), Lingtai (Ding and Yang, 2000), and Lantian (black: Kaakinen et al., 2006; purple: An et al., 2005). Dashed lines in (e–i) are modeled upper limits for $\delta^{13}C$ values of tooth enamel and soil carbonate formed in equilibrium with pure C_3 vegetation (Supplementary Table 1). For reference, $\delta^{13}C$ values for equilibrium with pure C_4 vegetation are ~+1.5 to +3.6‰ during this interval. (For interpretation of the references to colour in this figure legend, the reader is referred to the web version of this article.)

4.2.2. Latitudinal patterns of $\delta^{13}C$ in the loess plateau

The soil carbonate record from Baode is the most northerly CLP record published so far, and allows evaluation of latitudinal trends in soil carbonate $\delta^{13}C$ during late Neogene time. Data from Lantian (Kaakinen et al., 2006), Lingtai (An et al., 2005; Ding and Yang, 2000), and Xifeng (Jiang et al., 2002), along with the data from Baode, are shown in Figs. 4 and 5. Averaged over the late Miocene–early Pliocene interval [which we take here as 7–4 Ma, based on the approximate beginning of good spatial data coverage (7 Ma), and on the approximate beginning of pronounced changes in soil carbonate $\delta^{13}C$ values (4 Ma)], soil carbonate $\delta^{13}C$ is lowest in the south at Lantian (−9.8±0.6‰), and generally increases northward as shown by values at Lingtai (−8.3±0.5‰), Xifeng (−5.9±0.5‰) and Baode (−6.3±0.7‰). This pattern of northward-increasing $\delta^{13}C$ contrasts with patterns of southward increasing $\delta^{13}C$ of soil organic matter observed during the present day (An et al., 2005), and late Pleistocene (Liu et al., 2005) (Fig. 5c), which reflect southward-increasing abundance of C_4 vegetation in this region.

The northward-increasing $\delta^{13}C$ of soil carbonates during the 7–4 Ma interval may be related to one or a combination of two different end member scenarios:

1. *C_3 ecosystem scenario*. In this scenario, pure C_3 ecosystems characterized the CLP during this 7–4 Ma, and the $\delta^{13}C$ pattern is a record of northward-decreasing soil respiration rates due to increasing aridity, northward-increasing carbon isotope discrimination due to increasingly arid growth conditions, or northward-increasing incomplete leaching of parent material carbonate with a typical marine composition ($\delta^{13}C \approx -5$ to +2‰, $\delta^{18}O \approx -2$ to +2‰), or a combination of these.

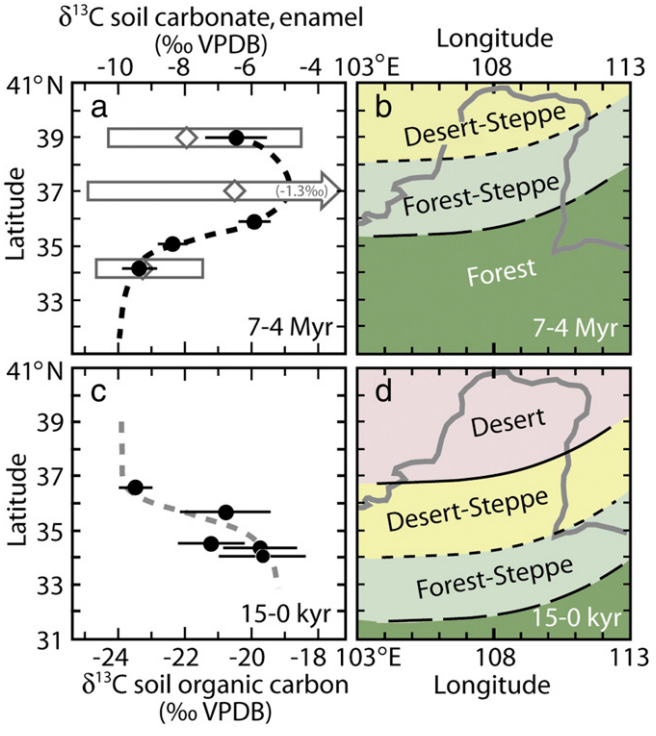

Fig. 5. Latitudinal changes in soil carbon $\delta^{13}C$ in the Chinese Loess Plateau and inferred vegetation distributions. (a) $\delta^{13}C$ values of soil carbonates (black circles with 1σ error bars) averaged over the period 7–4 Ma. From north to south the data are from Baode (this study; Supplementary Table 3), Xifeng (Jiang et al., 2002), Lingtai (Ding and Yang, 2000), and Lantian (Kaakinen et al., 2006). Tooth enamel $\delta^{13}C$ values dating between 6.5 and 5.5 Ma are shown by gray rectangles (range) and diamonds (average). (b) Inferred average position of the forest-steppe-desert transition during 7–4 Ma ago. (c) average $\delta^{13}C$ values (1σ error bars) of soil organic matter from soils post-dating 15 kyr. From north to south the data are from Huanxian, Xifeng, Xunyi, Weinan, and Lantian (Liu et al., 2005). (d) Inferred average position of the forest-steppe-–desert transition in nonmontane terrain during late Pleistocene to recent time.

Rao et al. (2006) show that such factors may have been important in late Pleistocene loess units that underwent minimal pedogenic alteration.

2. *Mixed C_3/C_4 ecosystem scenario*. In this scenario, soil respiration rates were relatively high, resetting of parent material compositions was thorough, increased carbon isotope discrimination was not a factor, and the $\delta^{13}C$ pattern represents actual changes from C_3-based ecosystems in the south to an increasing importance of C_4 vegetation in the north. This scenario implies northward-increasing C_4 vegetation in the Loess Plateau during 7–4 Ma, a pattern opposite of that observed today.

Tooth enamel data might shed light on which scenario more accurately describes actual conditions during the 7–4 Ma interval. Tooth enamel has an advantage over soil carbonate in that the plant-mineral fractionation is largely similar within broad classes of animals such as ungulate herbivores (see Cerling and Harris, 1999), and is not susceptible to factors such as low soil respiration rate and parent material carbonate contamination that can complicate interpretation of soil carbonate data. Tooth enamel from taxa dating between 6.5 and 5.5 Ma show a latitudinal trend similar to that of the soil carbonates (Fig. 5a). (This time interval is chosen because it is the only one during which all three sample regions are represented.) Tooth enamel unequivocally indicates the presence of C_4 vegetation in the Loess Plateau during the late Miocene and subsequent time. The first scenario is ruled out (pure C_3 ecosystems), and actual conditions may have been similar to those suggested by the second scenario (northward increasing importance of C_4 vegetation), or they may have been intermediate between these scenarios, with part of the northward increase in $\delta^{13}C$ due to increasing C_4 vegetation, and part due to more arid climates and lower soil productivity.

4.3. A humid late Miocene–early Pliocene climate?

4.3.1. Northward displacement of the forest-steppe-desert transition

The possibility of northward increasing C_4 vegetation in the Loess Plateau during ~7–4 Ma is intriguing and warrants further discussion, especially because C_4 vegetation generally decreases poleward, not only the Loess Plateau, but elsewhere globally as a result of cooler temperatures at higher latitudes. Studies thus far of C_4 vegetation in the Loess Plateau associate periods of increased abundance of C_4 vegetation with periods of increased summer monsoon strength.

Alternatively, patterns of C_4 vegetation can be interpreted in the context of a full forest-steppe-desert transition similar to that found in China today (Hou, 1983). In southeastern China, high precipitation allows existence of deciduous and evergreen forests, and these have a C_3 ecosystem carbon isotope signature. As precipitation decreases to the north, ecosystems open to forest-steppe, and then steppe or steppe-desert, with C_3 and C_4 grasses present in the open patches. Here, soil carbon reflects a mixture of C_3 and C_4 vegetation, as observed in the southern Loess Plateau today. Further northward, precipitation levels decrease, as do growing season temperatures, and mixed C_3-C_4 desert-steppe and desert predominate (Pyankov et al., 2000). Across this full vegetation transition, C_4 plants have a maximum abundance in the intermediate-monsoon-strength steppe environments. This 'steppe C_4 maximum' is bounded by C_3 monsoon forests to the south, and C_3 + C_4 deserts to the north.

We suggest that the ~7–4 Ma pattern of northward increasing C_4 vegetation can be explained by a northward shift in the average position of the forest-steppe-desert transition relative to its modern position, as illustrated in Fig. 5. Under this interpretation, Lantian and Lingtai were primarily woody ecosystems during this time, thus explaining the C_3 isotope signatures observed there, and the steppe-C_4 maximum was located north of these localities. The most parsimonious explanation for northward-displaced forests is higher effective humidity, with fire and herbivore pressure likely playing additional roles in regulating the amount of woody vegetation below upper limits dictated by rainfall amount (Bond and Keeley, 2005; Sankaran et al., 2005). The directionality of this humidity gradient is similar to that of the modern EAM, and sedimentological and geochemical evidence also indicate a similar directionality (Han et al., 2007).

Starting around 4 Ma and continuing to 2 Ma, the time-averaged position of the forest-steppe-desert transition retreated to the south, moving the C_4 maximum zone through the Lingtai and Lantian localities, and thus accounting for the peak in C_4 vegetation seen in these records centered around 2.7 Ma (Ding and Yang, 2000; Jiang et al., 2002; An et al., 2005). This time period corresponds to the transition from red clay strata to loess–paleosol strata, increased strength of the winter monsoons, and intensification of Northern Hemisphere glaciation (An et al., 2001).

Following ~2 Ma, we suggest that the time-averaged position of the steppe C_4 maximum resided near or to the south of the southern CLP. This model would predict northward-decreasing $\delta^{13}C$ values due to decreasing C_4 vegetation to the north, or, alternatively, relatively constant $\delta^{13}C$ values to the north if C_4 vegetation was an important component of desert vegetation, or if aridity-associated factors became more important to the north, including incomplete leaching, low respiration rates, or low ^{13}C discrimination by C_3 plants (*sensu* Rao et al., 2006). Although there are only two soil carbonate $\delta^{13}C$ records spanning this interval, Lantian and Lingtai (Fig. 4h and i, respectively), these show a slight decrease in average $\delta^{13}C$ values to the north and are consistent with the model described here.

On glacial–interglacial time scales during the Pleistocene, $\delta^{13}C$ analysis of soil organic matter indicates that the relative abundance of C_3 vegetation in the southern CLP increased during glacial intervals, apparently in response to cooler temperatures and weakened summer monsoons (An et al., 2005; Liu et al., 2005). We suggest that prior to ~4 Ma, the C_3-dominant ecosystems in the southern CLP comprised largely woody vegetation under relatively strong summer monsoon regimes, whereas following this time, periods of C_3-dominant ecosystems reflected increases in the relative abundance of C_3 grass over C_4 grass during glacial periods.

The Yushe tooth enamel record spans 6.2–2 Ma, and indicates that diets ranged between pure C_3 and ~60% C_4 throughout the interval. This suggests that Yushe remained a mixed woody–grassy ecosystem during this time, offering sufficient graze and browse foodstuffs to support respective grazing and browsing taxa.

If Yushe were indeed more forested during 7–4 Ma compared to the ensuing interval, as we suggest above, then it might be expected that tooth enamel $\delta^{13}C$ values would be correspondingly lower during 7–4 Ma due to primarily C_3 browsing diets, and higher afterwards as more C_4 grass became available. However, it must be considered that large mammalian herbivores are selective in their dietary intake, and largely separate into browsing and grazing specialties. Therefore, in order for tooth enamel isotopes to accurately portray the abundance of C_3 versus C_4 vegetation in an ecosystem, the selection of specimens of different species for isotopic analysis would have to closely mirror the abundance of those species when they were extant. Accurate taxonomic abundance estimates are difficult to achieve (or verify) for fossil assemblages, and this type of paleontological work remains to be realized at Yushe. Therefore, we do not suggest that our tooth enamel isotopic data at Yushe are reflective of actual C_3 versus C_4 abundance; rather they serve as an indication that both C_3 and C_4 plants were available to herbivores during the entire 6.2–2 Ma interval represented by our data.

4.3.2. Independent evidence of a relatively humid 7–4 Ma interval in the Loess Plateau

There is a growing body of evidence suggestive of, or consistent with, relatively humid climates during the 7–4 Ma interval in the CLP, and particularly during the early Pliocene (~5.3–4 Ma). This evidence, discussed below, centers on interpretations of the lithology of the red

clay, mollusk faunas, herbivore faunas, pollen, and the dust flux record in the North Pacific.

Detailed studies of grain size and pedostratigraphy of the red clay indicate that it experienced a greater degree of pedogenesis than the overlying loess–soil deposits (Ding et al., 1999; Sun et al., 2006). In particular, Ding et al. (1999) identify extremely mature soils in the 5.2–3.85 Ma interval at Lingtai, and interpret these as indicating warm and wet climates, and possibly the strongest summer monsoons in the past 7 Ma. At Baode, the interval immediately following 5.3 Ma is similarly well developed, with fine-scale ped structure, clay skins, and Fe–Mn stains, and thorough leaching of matrix carbonate. Isolated carbonate horizons are extensively dissolved and recrystallized, suggesting a high throughput of meteoric water following drier intervals during which the carbonate formed. At Xifeng, grain-size 'U-ratios' of red clay sediment (16–44 μm/5.5–16 μm) are relatively low between 5.36 and 3.5 Ma, a pattern interpreted by Vandenberghe et al. (2004) to represent warm conditions and weak winter monsoons.

Fossil mollusk communities were studied at Xifeng by Wu et al. (2006). Their record, spanning 6.2–2.4 Ma, shows a predominance of thermo-humidiphilous and meso-xerophilous mollusks between 5.4 and 3.5 Ma, and a near absence of cold-aridiphilous mollusks during this time. This later group, however, is abundant 5.5–5.9 Ma, and again following 3.5 Ma. Thermo-humidiphilous taxa are found today in southeast China where mean annual temperatures (MAT) are 13–17.5 °C and mean annual precipitation (MAP) is 620–1120 mm. Meso-xerophilous taxa are associated with MATs of 6–12 °C and MAPs of 400–800 mm, and the cold-aridiphilous taxa are associated with MATs of 5.8–10.5 °C and MAPs of 200–450 mm (Wu et al., 2006). Xifeng today has a MAT of ~9 °C and a MAP of 585 mm, so the presence of thermo-humidiphilous mollusk taxa during 5.4–3.5 Ma is consistent with warmer temperatures and higher precipitation during that interval. A more recent molluscan record from the CLP confirms the suggestion of relatively humid conditions during 5.1 to 4 Ma, and more arid conditions in the preceding 7.1 to 5.5 Ma interval (Li et al., 2008).

Late Miocene herbivore faunas in northern China have long been recognized as having steppe, forest, or mixed aspects (Schlosser, 1903; Kurtén, 1952), and fossil tooth morphology suggests that a large portion of the taxa were browsers and therefore occupied habitats in which woody vegetation was abundant. Recent reevaluations support these interpretations (Fortelius et al., 2002; Zhang, 2006), and suggest that on a global scale, the late Miocene in northern China was a period of relatively humid climate, whereas the late Miocene was a period of drying elsewhere in Eurasia (Fortelius and Zhang, 2006). At Baode, cervids and gazelles with low tooth crown heights consumed pure C_3 vegetation, consistent with a browsing diet, whereas higher-crowned *Urmiatherium* and yet higher-crowned *Hipparion* consumed some C_4 vegetation (this study, and Passey et al., 2007). Except for *Hipparion*, few of the taxa have tooth morphologies characteristic of modern grazers in grassland ecosystems. In addition, mesowear analysis (Fortelius and Solounias, 2000) of late Miocene herbivores from across the CLP suggests that browsing and mixed feeding diets were far more common than pure grazing diets (Fortelius, Eronen, and Liu, unpublished data). Overall, this signature is consistent with mixed woody and grassy ecosystems at Baode during the late Miocene, and a northward-displaced forest-steppe-desert transition during that time.

Pollen data from Xifeng (Wang et al., 2006) span 6.2–2.4 Ma, and show relatively high percentages of arboreal taxa between 6.2 and 4.2 Ma (~20–40%), including *Pinus*, *Betula*, and *Quercus*. Pollen from these taxa was significantly lower after 4.2 Ma (~5–20%). Grass and *Artemisia* pollen are also predominant during 6.2–4.2 Ma (~10–20%, and 20–50%, respectively), suggesting a forest-steppe habitat. Following 4.2 Ma, the abundance of tree pollen decreases, grass and *Artemisia* stay essentially the same, and Chenopods increase, consistent with a southward displacement of the forest-steppe-desert transition. The pollen record to the south at Chaona (Ma et al., 2005) contains significantly higher percentages of arboreal taxa than at Xifeng. Arboreal taxa including those listed above, as well as *Cedrus*, *Tsuga*, and *Juniperus*, comprise ~50% of the pollen spectrum for much of the interval between 8.1 and 3.7 Ma, and reach 70–80% during some periods. Grasses and *Artemisia* are common, again suggesting a mixed forest steppe habitat. Elevated arboreal pollen at Chaona compared to Xifeng is consistent with southward increasing forest vegetation and the general vegetation model depicted in Fig. 5b. It should be noted that Ma et al. (2005) suggest, by analogy with the present day vegetation and topography, a montane origin for some of the arboreal taxa observed in their pollen record. A sharp increase in arboreal taxa dominated almost exclusively by Cupressacae and *Juniperus* occurs at 3.7 Ma, which the authors ascribe to an enhancement of monsoon-related climatic seasonality.

Finally, the dust flux record at site 885/886 in the North Pacific (Rea et al., 1998) is downwind of northern China, and may provide insight about ancient climates there. The record contains three predominant features: an abrupt peak in dust flux 8–7 Ma, a low dust flux ~7–4 Ma (with extremely low levels 5.2–4.2 Ma), and permanently increased dust flux after 4 Ma. The peak at 8–7 Ma predates the time period for which we have a good latitudinal record of C_4 vegetation in the Loess Plateau. However, the decreased dust flux during 7–4 Ma is consistent with the suggestion of relatively humid climates in the Loess Plateau, and suppression of dust from potential source areas. Especially intriguing is the fact that the very humid climates between 5.3 and 3.85 Ma suggested by extremely well-developed red clay soils (Ding et al., 1999) are broadly coincident with the period of lowest dust flux in the North Pacific. We also point out that a permanent increase in dust flux following ~4 Ma is consistent with the notion, outlined above, of a permanent retreat of the forest-steppe-desert transition (and the steppe-C_4 maximum zone) at this time. Indeed, the suggestion (An et al., 2005) that the summer monsoon became stronger during this time period as evidenced by C_4 expansion was originally correlated to the increased North Pacific dust flux at this time. However, after ~2.5 Ma, C_4 biomass decreased in the southern Loess Plateau, while the dust flux remained high. The suggestion presented here—that the forest-steppe-desert transition zone retreated to the south during 4–2 Ma, thus imparting transient C_4 maximum signals at Xifeng, Lingtai, and Lantian—reconciles this paradox because permanent regional drying at this time is consistent with a permanent increase in North Pacific dust flux.

4.4. Implications for forcing mechanisms of the East Asian monsoons

The inferred pattern of enhanced humidity in northern China during the late Miocene and early Pliocene, and the subsequent aridification leading into the Pleistocene, are in keeping with the current state of knowledge about the long-term dynamics of the EAM. A tight phasing exists between Northern Hemisphere climates and the EAM at both orbital and suborbital timescales (Wang et al., 2008), consistent with the notion that changes in high latitude warmth, snow and ice cover, and insolation—whether orbital or nonorbital in origin—are related to changes in monsoon dynamics. Southward migration of zonal patterns such as the Siberian High and related low-index Northern Hemisphere annular mode conditions (Thompson and Wallace, 2001) during cold stages provides a widely recognized first-order link between glacial climates and strengthened EAWM. It has further been suggested that the EASM is weakened by the opposing influence of the EAWM (Liu and Ding, 1998), and that it perhaps strengthened with persistent El Niño modes during the Holocene (Hong et al., 2005). Recent modeling studies suggest that changes in vegetation cover in Tibet and in the high latitudes have a significant impact on monsoon dynamics (Zheng et al., 2004; Yasunari et al., 2006), with more extensive cover in these regions generally promoting increased summer monsoon precipitation. The seasonal-, suborbital-, and orbital-, and supra-orbital-scale relationship between high-latitude warmth and

summer monsoons is well documented (Liu and Ding, 1998; Wang et al., 2008), and it now appears that the mechanism driving this relationship transcends the current 'Ice Age' climatic state and has operated for the past several million years.

It is known that a high elevation Tibetan Plateau is a key element driving strong EASM (Kutzbach et al., 1993; An et al., 2001; Zhang et al., 2007). Though the surface elevation history of the Tibetan Plateau is a matter of ongoing debate (Molnar, 2005), most data suggest that relatively high elevations (>3000 m) were attained at least by the late Miocene. Thus, humid climates of northern China during the late Miocene and early Pliocene may have existed under a favorable combination of sufficiently high Tibetan Plateau elevations, and relatively warm conditions in the high latitude Northern Hemisphere. Both factors would have acted to enhance humidity and thereby create a remarkable regional reversal of the global trend of mid-latitude drying following the middle Miocene (Fortelius et al., 2002).

5. Conclusions

Tooth enamel data in this paper show that C_4 vegetation has been present in China since the late Miocene, a finding that contrasts with previous notions of a delayed C_4 expansion in China compared to other regions globally. Therefore, the idea of a global late Miocene C_4 event remains valid. The spatial pattern of C_4 vegetation during the late Neogene is consistent with a monsoon climate system forcing humid conditions in the southeast, and more arid conditions in the northwest.

Latitudinal trends in soil carbonate $\delta^{13}C$ reveal further details about late Neogene climate in China. During the ~7–4 Ma interval, $\delta^{13}C$ values show a northward-increasing pattern opposite in direction to that observed during subsequent time and today. The 7–4 Ma $\delta^{13}C$ pattern is likely due to northward increasing C_4 vegetation, possibly combined with northward increasing aridity causing lower soil respiration rates, increased carbon isotope discrimination in C_3 plants, or incomplete isotopic resetting of parent material carbonate. We suggest that the 7–4 Ma pattern can be explained by a northward displacement of the forest-steppe-desert transition zone relative to its modern position, which implies that climate was relatively humid during this interval. The suggestion of a humid 7–4 Ma climate is consistent with a number of proxy data, including red clay lithology, mammal and mollusk faunas, pollen records, and dust flux in the North Pacific. A permanent retreat of this zone during 4–2 Ma explains the transient increase in C_4 vegetation observed at southern Loess Plateau localities, and is consistent with onset of strong winter monsoons and permanently increased dust flux in the North Pacific at this time.

An important aspect of our model is that soil carbonate $\delta^{13}C$ values indicative of C_3-dominated ecosystems are not necessarily indicative of weak summer monsoon conditions: a C_3 signal may equally well derive from woody ecosystems existing under strong monsoon conditions, as from steppe and desert ecosystems existing under weak monsoon conditions. We suggest that, at the latitudes of the Chinese Loess Plateau, and under a monsoonal climatic regime, the ecological viability of C_4 vegetation is limited in the south by warm-humid conditions more favorable to C_3 forest, and in the north by cold-dry conditions more favorable to C_3 steppe and desert.

The interpretation of relatively humid conditions during the late Miocene and early Pliocene implies that a 'warm high latitude/strong summer monsoon' association characteristic of the Pleistocene EAM system existed prior to the Plio-Pleistocene climatic reorganization. This supports the idea that a long-lived feature of the Eurasian system, likely the continental and orographic configuration, provides the framework or catalyst necessary for the existence of the EAM (Kutzbach et al., 1993). Superimposed on this framework are transient features such as snow, ice, and vegetation cover, sea-surface temperatures, and solar insolation. In northern China, these transient features appear to exert the primary forcing that controls the balance between humid EASM-dominated climates, and arid EAWM-dominated climates.

Acknowledgments

We thank L.P. Liu, T. Jokela, A. Karme, W. Zhou, and J. Peel for providing assistance with field, laboratory, and museum work. We are grateful to the Academy of Finland, the National Geographic Society, National Science Foundation China, National Science Foundation USA, the Packard Foundation, the Geological Society of America, and the Associated Students of the University of Utah for providing the funding. We thank David Rea, Yang Shiling, and Jiang Wenying for sharing electronic files of previously published data, and Larry Flynn for reviewing the Yushe chronology. We thank Han Jintai and an anonymous reviewer for providing comments and criticisms that helped to improve the clarity of this paper.

Appendix A. Supplementary data

Supplementary data associated with this article can be found, in the online version, at doi:10.1016/j.epsl.2008.11.008.

References

An, Z.S., 2000. The history and variability of the East Asian paleomonsoon climate. Quat. Sci. Rev. 19, 171–187.
An, Z.S., Wang, S.M., Wu, X.H., Chen, M.Y., Sun, D.H., Liu, X.M., Wang, F.B., Li, L., Sun, Y.B., Zhou, W.J., Zhou, J., Liu, X.D., Lu, H.Y., Zhang, Y.X., Dong, G.G., Qiang, X.K., 1999. Eolian evidence from the Chinese Loess Plateau: the onset of the Late Cenozoic Great Glaciation in the Northern Hemisphere and Qinghai–Xizang Plateau uplift forcing. Sci. China Ser. D-Earth Sci. 42, 258–271.
An, Z.S., Kutzbach, J.E., Prell, W.L., Porter, S.C., 2001. Evolution of Asian monsoons and phased uplift of the Himalaya-Tibetan plateau since Late Miocene times. Nature 411, 62–66.
An, Z.H., Huang, Y.S., Liu, W.G., Guo, Z.T., Clemens, S., Li, L., Prell, W., Ning, Y.F., Cai, Y.J., Zhou, W.J., Lin, B.H., Zhang, Q.L., Cao, Y.N., Qiang, X.K., Chang, H., Wu, Z.K., 2005. Multiple expansions of C_4 plant biomass in East Asia since 7 Ma coupled with strengthened monsoon circulation. Geology 33, 705–708.
Bailey, R.G., 1989/1993. Bailey ecoregions of the continents (reprojected) from the World Conservation Monitoring Center. Global Ecosystems Database Version 2.0. NOAA National Geophysical Data Center, Boulder, CO. http://www.ngdc.noaa.gov/seg/cdroms/ged_iib/datasets/b03/bec.htm (Downloaded August 2006).
Bloemendal, J., Liu, X.M., Sun, Y.B., Li, N.N., 2008. An assessment of magnetic and geochemical indicators of weathering and pedogenesis at two contrasting sites on the Chinese Loess Plateau. Palaeogeogr. Palaeoclimatol. Palaeoecol. 257, 152–168.
Bond, W.J., Keeley, J.E., 2005. Fire as a global 'herbivore.' The ecology and evolution of flammable ecosystems. Trends Ecol. Evol. 20, 387–394.
Cerling, T.E., 1984. The stable isotopic composition of modern soil carbonate and its relationship to climate. Earth Planet. Sci. Lett. 71, 229–240.
Cerling, T.E., Harris, J.M., 1999. Carbon isotope fractionation between diet and bioapatite in ungulate mammals and implications for ecological and paleoecological studies. Oecologia 120, 347–363.
Cerling, T.E., Harris, J.M., MacFadden, B.J., Leakey, M.G., Quade, J., Eisenmann, V., Ehleringer, J.R., 1997. Global vegetation change through the Miocene/Pliocene boundary. Nature 389, 153–158.
Chen, J., An, Z.S., Head, J., 1999. Variation of Rb/Sr ratios in the loess–paleosol sequences of central China during the last 130,000 years and their implications for monsoon paleoclimatology (vol 51, pg 215, 1999). Quat. Res. 52, 269-269.
Deng, T., Dong, J., Wang, Y., 2002. Variation of terrestrial ecosystem recorded by stable carbon isotopes of fossils in northern China during the Quaternary. Chin. Sci. Bull. 47, 76–78.
Ding, Z.L., Yang, S.L., 2000. C_3/C_4 vegetation evolution over the last 7.0 Myr in the Chinese Loess Plateau: evidence from pedogenic carbonate $\delta^{13}C$. Palaeogeogr. Palaeoclimatol. Palaeoecol. 160, 291–299.
Ding, Z.L., Sun, J.M., Liu, T.S., Zhu, R.X., Yang, S.L., Guo, B., 1998. Wind-blown origin of the Pliocene red clay formation in the central Loess Plateau, China. Earth Planet. Sci. Lett. 161, 135–143.
Ding, Z.L., Xiong, S.F., Sun, J.M., Yang, S.L., Gu, Z.Y., Liu, T.S., 1999. Pedostratigraphy and paleomagnetism of a ~7.0 Ma eolian loess-red clay sequence at Lingtai, Loess Plateau, north-central China and the implications for paleomonsoon evolution. Palaeogeogr. Palaeoclimatol. Palaeoecol. 152, 49–66.
Dowsett, H., Thompson, R., Barron, J., Cronin, T., Fleming, F., Ishman, S., Poore, R., Willard, D., Holtz, T., 1994. Joint investigations of the middle Pliocene climate 1: PRISM paleoenvironmental reconstructions. Glob. Planet. Change 9, 169–195.
Ehleringer, J.R., Cerling, T.E., Helliker, B.R., 1997. C_4 photosynthesis, atmospheric CO_2, and climate. Oecologia 112, 285–299.
Flynn, L.J., Wu, W., Downs, W.R., 1997. Dating vertebrate microfaunas in the late Neogene record of Northern China. Palaeogeogr. Palaeoclimatol. Palaeoecol. 133, 227–242.

Fortelius, M., Solounias, N., 2000. Functional characterization of ungulate molars using the abrasion-attrition wear gradient: a new method for reconstructing paleodiets. Amer. Mus. Nov. 3301, 1–36.
Fortelius, M., Zhang, Z.Q., 2006. An oasis in the desert? History of endemism and climate in the late Neogene of North China. Palaeontogr. Abt. A: Palaozool., Stratigr. 227, 131–141.
Fortelius, M., Eronen, J., Jernvall, J., Liu, L.P., Pushkina, D., Rinne, J., Teaskov, A., Vislobokova, I., Zhang, Z.Q., Zhou, L.P., 2002. Fossil mammals resolve regional patterns of Eurasian climate change over 20 million years. Evol. Ecol. Res. 4, 1005–1016.
Gaboardi, M., Deng, T., Wang, Y., 2005. Middle Pleistocene climate and habitat change at Zhoukoudian, China, from the carbon and oxygen isotopic record from herbivore tooth enamel. Quat. Res. 63, 329–338.
Gile, L.H., Peterson, F.F., Grossman, R.B., 1966. Morphological and genetic sequences of carbonate accumulation in desert soils. Soil Sci. 101, 347–360.
Guo, Z.T., Ruddiman, W.F., Hao, Q.Z., Wu, H.B., Qiao, Y.S., Zhu, R.X., Peng, S.Z., Wei, J.J., Yuan, B.Y., Liu, T.S., 2002. Onset of Asian desertification by 22 Myr ago inferred from loess deposits in China. Nature 416, 159–163.
Han, J.T., Chen, H.H., Fyfe, W.S., Guo, Z.F., Wang, D.J., Liu, T.S., 2007. Spatial and temporal patterns of grain size and chemical weathering of the Chinese Red Clay Formation and implications for East Asian monsoon evolution. Geochim. Cosmochim. Acta 71, 3990–4004.
Hao, Q.Z., Guo, Z.T., 2005. Spatial variations of magnetic susceptibility of Chinese loess for the last 600 kyr: implications for monsoon evolution. J. Geophys. Res. 110, B12101.
Hong, Y.T., Hong, B., Lin, Q.H., Shibata, Y., Hirota, M., Zhu, Y.X., Leng, X.T., Wang, Y., Wang, H., Yi, L., 2005. Inverse phase oscillations between the East Asian and Indian Ocean summer monsoons during the last 12000 years and paleo-El Niño. Earth Planet. Sci. Lett. 231, 337–346.
Hou, H.Y., 1983. Vegetation of China with reference to its geographical distribution. Annal. Missouri Botanic. Gardens 70, 509–548.
Imbrie, J., Boyle, E.A., Clemens, S.C., Duffy, A., Howard, W.R., Kukla, G., Kutzbach, J., Martinson, D.G., McIntyre, A., Mix, A.C., Molfino, B., Morley, J.J., Peterson, L.C., Pisias, N.G., Prell, W.L., Raymo, M.E., Shackleton, N.J., Toggweiler, J.R., 1992. On the structure and origin of major glaciation cycles. 1. Linear responses to Milankovitch forcing. Paleoceanography 7, 701–738.
Jiang, W.Y., Peng, S.Z., Hao, Q.Z., Liu, D.S., 2002. Carbon isotopic records in paleosols over the Pliocene in Northern China: implication on vegetation development and Tibetan uplift. Chin. Sci. Bull. 47, 687–690.
Kaakinen, A., 2005. A long terrestrial sequence in Lantian—a window into the late Neogene paleoenvironments of northern China. Publications of the Department of Geology, D4. Helsinki, pp. 1–49.
Kaakinen, A., Lunkka, J.P., 2003. Sedimentation of the Late Miocene Bahe Formation and its implications for stable environments adjacent to Qinling mountains in Shaanxi, China. J. Asian Earth Sci. 22, 67–78.
Kaakinen, A., Sonninen, E., Lunkka, J.P., 2006. Stable isotope record in paleosol carbonates from the Chinese Loess Plateau: implications for late Neogene paleoclimate and paleovegetation. Palaeogeogr. Palaeoclimatol. Palaeoecol. 237, 359–369.
Koch, P.L., 1998. Isotopic reconstruction of past continental environments. Annu. Rev. Earth Planet. Sci. 26, 573–613.
Kohn, M.J., Cerling, T.E., 2002. Stable isotope compositions of biological apatite. Phosphates: Geochemical, Geobiological, and Materials Importance, 48, pp. 455–488.
Kurtén, B., 1952. The Chinese Hipparion fauna. Commentationes Biologicae, Societas Scientiarum Fennica, 13, pp. 1–82.
Kutzbach, J.E., Prell, W., Ruddiman, W.F., 1993. Sensitivity of Eurasian climate to surface uplift of the Tibetan Plateau. J. Geol. 101, 177–190.
Li, F.J., Rousseau, D.-D., Wu, N.Q., Hao, Q.Z., Pei, Y.P., 2008. Late Neogene evolution of the East Asian monsoon revealed by terrestrial mollusk record in Western Chinese Loess Plateau: from winter to summer dominated sub-regime. Earth Planet. Sci. Lett. 274, 439–447.
Liu, T.S., Ding, Z.L., 1998. Chinese loess and the paleomonsoon. Annu. Rev. Earth Planet. Sci. 26, 111–145.
Liu, W.G., Huang, Y.S., An, Z.S., Clemens, S.C., Li, L., Prell, W.L., Ning, Y.F., 2005. Summer monsoon intensity controls C_4/C_3 plant abundance during the last 35 ka in the Chinese Loess Plateau: Carbon isotope evidence from bulk organic matter and individual leaf waxes. Palaeogeogr. Palaeoclimatol. Palaeoecol. 220, 243–254.
Ma, Y.Z., Wu, F.L., Fang, X.M., Li, J.J., An, Z.S., Wang, W., 2005. Pollen record from red clay sequence in the central Loess Plateau between 8.10 and 2.60 Ma. Chin. Sci. Bull. 50, 2234–2243.
Machette, M.N., 1985. Calcic soils in the southwestern United States. In: Weide, D.L. (Ed.), Soils and Quaternary Geology of the Southwestern United States. Geological Society of America, Boulder, CO, pp. 1–22.
Mix, A.C., Pisias, N.G., Rugh, W., Wilson, J., Morey, A., Hagelberg, T.K., 1995. Benthic foraminifer stable isotope record from Site 849 (0–5 Ma): local and global climate changes. In: Pisias, N.G., Mayer, L.A., Janecek, T.R., Palmer-Julson, A., Van Andel, T.H. (Eds.), Proc. ODP Sci. Results, p. 138.
Molnar, P., 2005. Mio-Pliocene growth of the Tibetan Plateau and evolution of East Asian climate. Palaeontol. Electronica 8 (1), 2A.
Passey, B.H., Cerling, T.E., Perkins, M.E., Voorhies, M.R., Harris, J.M., Tucker, S.T., 2002. Environmental change in the Great Plains: an isotopic record from fossil horses. J. Geol. 110, 123–140.
Passey, B.H., Eronen, J.T., Fortelius, M., Zhang, Z.Q., 2007. Paleodiets and paleoenvironments of late Miocene gazelles from North China: evidence from stable carbon isotopes. Vertebrata PalAsiatica 45, 118–127.
Pyankov, V.I., Gunin, P.D., Tsoog, S., Black, C.C., 2000. C4 plants in the vegetation of Mongolia: their natural occurrence and geographical distribution in relation to climate. Oecologia 123, 15–31.
Qiu, Z.X., Qiu, Z.D., 1995. Chronological sequence and subdivision of Chinese Neogene mammalian faunas. Palaeogeogr. Palaeoclimatol. Palaeoecol. 116, 41–70.
Quade, J., Cater, J.M.L., Ojha, T.P., Adam, J., Harrison, T.M., 1995. Late Miocene environmental change in Nepal and the northern Indian subcontinent: stable isotopic evidence from paleosols. Geol. Soc. Amer. Bull. 107, 1381–1397.
Rao, Z.G., Zhu, Z.Y., Chen, F.H., Zhang, J.W., 2006. Does $\delta^{13}C_{carb}$ of the Chinese loess indicate past C_3/C_4 abundance? A review of research on stable carbon isotopes of the Chinese loess. Quat. Sci. Rev. 25, 2251–2257.
Ravelo, A.C., Anderson, D.K., Lyle, M., Lyle, A.O., Wara, M.W., 2004. Regional climate shifts caused by global cooling in the Pliocene epoch. Nature 429, 263–267.
Rea, D.K., Snoeckx, H., Joseph, L.H., 1998. Late Cenozoic eolian deposition in the North Pacific: asian drying, Tibetan uplift, and cooling of the northern hermisphere. Paleoceanography 13, 215–224.
Sankaran, M., et al., 2005. Determinants of woody cover in African savannas. Nature 438, 846–849.
Schlosser, M., 1903. Die fossilen Saugethiere Chinas nebst einer odontographie der recenten antilopen. Abhandlungen der Koniglichen Bayerischen Akademie der Wissenschaften, 22, pp. 1–221.
Sun, X.J., Wang, P.X., 2005. How old is the Asian monsoon system?—Palaeobotanical records from China. Palaeogeogr. Palaeoclimatol. Palaeoecol. 222, 181–222.
Sun, Y.B., Lu, H., An, Z.S., 2006. Grain size of loess, palaeosol and Red Clay deposits on the Chinese Loess Plateau: significance for understanding pedogenic alteration and palaeomonsoon evolution. Palaeogeogr. Palaeoclimatol. Palaeoecol. 241, 129–138.
Tedford, R.H., Flynn, L.J., Qiu, Z.X., Opdyke, N.D., Downs, W.R., 1991. Yushe Basin, China: paleomagnetically calibrated mammalian biostratigraphic standard for the late Neogene of eastern Asia. J. Vertebr. Paleontol. 11, 519–526.
Teeri, J.A., Stowe, L.G., 1976. Climatic patterns and the distribution of C4 grasses in North America. Oecologia 23, 1–12.
Thompson, D.W.J., Wallace, J.M., 2001. Regional climate impacts of the Northern Hemisphere annular mode. Science 293, 85–89.
UCAR, 2006. China Monthly Station Precipitation and Temperature, 1951–1990. http://dss.ucar.edu/datasets/ds578.1. Downloaded 9-August-2006.
Vandenberghe, J., Lu, H.Y., Sun, D.H., van Huissteden, J., Konert, M., 2004. The late Miocene and Pliocene climate in East Asia as recorded by grain size and magnetic susceptibility of the Red Clay deposits (Chinese Loess Plateau). Palaeogeogr. Palaeoclimatol. Palaeoecol. 204, 239–255.
Wang, Y., Deng, T., 2005. A 25 m.y. isotopic record of paleodiet and environmental change from fossil mammals and paleosols from the NE margin of the Tibetan Plateau. Earth Planet. Sci. Lett. 236, 322–338.
Wang, Y., Cerling, T.E., MacFadden, B.J., 1994. Fossil horses and carbon isotopes: new evidence for Cenozoic dietary, habitat, and ecosystem changes in North America. Palaeogeogr. Palaeoclimatol. Palaeoecol. 241, 118–128.
Wang, L., Lu, H.Y., Wu, N.Q., Li, J., Pei, Y.P., Tong, G.B., Peng, S.Z., 2006. Palynological evidence for Late Miocene–Pliocene vegetation evolution recorded in the red clay sequence of the central Chinese Loess Plateau and implication for palaeoenvironmental change. Palaeogeogr. Palaeoclimatol. Palaeoecol. 241, 118–128.
Wang, Y.J., Cheng, H., Edwards, R.L., Kong, X.G., Shao, X.H., Chen, S.T., Wu, J.Y., Jiang, X.Y., Wang, X.F., An, Z.S., 2008. Millenial- and orbital-scale changes in the East Asian monsoon over the past 224,000 years. Nature 451, 1090–1093.
West, A.G., Bond, W.J., Midgley, J.J., 2000. Soil carbon isotopes reveal ancient grassland under forest in Hluhluwe, KwaZulu-Natal. South Afr. J. Sci. 96, 252–254.
Wu, N.Q., Pei, Y.P., Lu, H.Y., Guo, Z.T., Li, F.J., Liu, T.S., 2006. Marked ecological shifts during 6.2–2.4 Ma revealed by a terrestrial molluscan record from the Chinese Red Clay Formation and implication for palaeoclimatic evolution. Palaeogeogr. Palaeoclimatol. Palaeoecol. 233, 287–299.
Yasunari, T., Saito, K., Takata, K., 2006. Relative roles of large-scale orography and land surface processes in the global hydroclimate. Part I: Impacts on monsoon systems and the tropics. J. Hydrometeorol. 7, 626–641.
Zachos, J., Pagani, M., Sloan, L., Thomas, E., Billups, K., 2002. Trends, rhythms, and abberations in global climate 65 Ma to present. Science 292, 686–693.
Zhang, Z.Q., 2006. Chinese late Neogene land mammal community and the environmental changes of East Asia. Vertebrata Palasiatica 44, 133–142.
Zhang, Z.S., Wang, H.J., Guo, Z.T., Jiang, D.B., 2007. Impact of tectonic changes on the reorganization of the Cenozoic paleoclimatic patterns in China. Earth Planet. Sci. Lett. 257, 622–634.
Zheng, Y.Q., Yu, G., Wang, S.M., Xue, B., Zhou, D.Q., Zeng, X.M., Liu, H.Q., 2004. Simulation of paleoclimate over East Asia at 6 ka BP and 21 ka BP by a regional climate model. Clim. Dyn. 23, 513–529.
Zhu, Y.M., Zhou, L.P., Mo, D.W., Kaakinen, A., Zhang, Z.Q., Fortelius, M., 2008. A new magnetostratigraphic framework for late Neogene Hipparion Red Clay in the eastern Loess Plateau of China. Palaeogeogr. Palaeoclimatol. Palaeoecol. 268, 47–57.